Multi-dimensional Free-surface Multiple Elimination and Source Deblending of Volve OBC Data

Citation for published version:
Ravasi, M, Vasconcelos, I, Curtis, A & Kritski, A 2015, 'Multi-dimensional Free-surface Multiple Elimination and Source Deblending of Volve OBC Data' Paper presented at 77th EAGE Conference & Exhibition 2015, Madrid, Spain, 1/06/15 - 4/06/15, .

Th P2 05

Multi-dimensional Free-surface Multiple Elimination and Source Deblending of Volve OBC Data

M. Ravasi* (University of Edinburgh), I. Vasconcelos (Schlumberger Gould Research), A. Curtis (University of Edinburgh) & A. Kritski (Statoil)

SUMMARY

The wave-equation approach to signature deconvolution and free-surface related multiple elimination of multi-component ocean-bottom data of Amundsen (2001) has recently been linked to seismic interferometry by multi-dimensional deconvolution (MDD). When applied to simultaneous-source data this method can also unravel and reorganise blended data into sequential source responses. We have generated two blended versions of the Volve OBC dataset and compared the ability of MDD to deblend different types of simultaneous-source acquisitions together with suppressing free-surface multiples. Reverse-time migration of the deblended responses produces seismic images of similar quality to those from truly sequential source data.

Introduction

Many seismic data processing and migration methods are based on the assumption that seismic data only contain primary reflections. In ocean-bottom cable (OBC) data, water multiples generated from the sea surface, which acts as a perfect reflector, are strong and contaminate primary reflections. The attenuation of these events is required for seismic imaging using many standard methods of migration.

Multiple attenuation algorithms are often based on the fact that multiple energy mainly propagates downwards from the sea surface in the fluid and thus is down-going when recorded at a receiver on the seabed, whereas primary reflections propagate upwards from the subsurface to the receiver. One way to attenuate receiver ghosts and water column reverberations is to separate up and downgoing energy either explicitly by combining the geophone and hydrophone using the methods of PZ-summation (Barr and Sanders 1989; Soubaras, 1996) or implicitly during migration by jointly imaging pressure and velocity data via vector-acoustic migration (Vasconcelos, 2013; El Yadari and Hou, 2013; Ravasi et al., 2014).

On the other hand when the reflection on a subsurface reflector occurs after one or more reverberations in the water layer, the multiple events, usually called source-side multiples, are seen as up-going energy. The wave-equation approach of Amundsen (2001) can also suppress this type of free-surface related multiples by transforming the recorded ocean-bottom seismic data into a designatured data that would be recorded in a hypothetical seismic experiment with no sea surface present. The key is to solve an integral equation by means of multi-dimensional deconvolution (MDD) via, e.g., least-squares inversion (Wapenaar et al., 2011). Wapenaar et al. (2012) and Vasconcelos and Rickett (2013) have shown that if blended data are taken as input, MDD can also naturally deblend data recorded with simultaneous-source acquisition.

We have tested this approach on a OBC dataset from the Volve field in the North Sea, demonstrating that simultaneous-source data can be successfully deblended as well as free-surface multiples suppressed, and we have ultimately produced seismic images of similar quality to those from sequential source data.

Theory of wave-equation demultiple (and deblending)

The integral relationship between the recorded multi-component data in the physical ocean-bottom seismic experiment and the desired designatured data without free-surface is (Amundsen, 2001)

$$p^-(\mathbf{x}'_R,\mathbf{x}_S,\omega) = \int_{\partial D_R} p^+(\mathbf{x}_R,\mathbf{x}_S,\omega)\,R_0(\mathbf{x}_R,\mathbf{x}'_R,\omega)\,d\mathbf{x}_R. \qquad (1)$$

For each angular frequency ω, p^- and p^+ are the up- and down-going wavefields from sources $\mathbf{x}_S$ to receivers $\mathbf{x}_R$ (and $\mathbf{x}'_R$) recorded along the receiver array ∂D_R, respectively. The desired reflection response R_0 is a redatumed wavefield from dipole point sources $\mathbf{x}'_R$ to pressure receivers $\mathbf{x}_R$ with a water layer that extends upwards to infinity, and with the same geology of the physical experiment below ∂D_R. Recorded data may derive from sequential transient sources

$$p^\pm(\mathbf{x}_R,\mathbf{x}_S,\omega) = s(\omega)G^\pm(\mathbf{x}_R,\mathbf{x}_S,\omega) \qquad (2)$$

or from simultaneous sources (Wapenaar et al., 2012)

$$p^\pm(\mathbf{x}_R,\sigma_S,\omega) = \sum_{\mathbf{x}_S^{(i)}\in\sigma_S} s^{(i)}(\omega)e^{-j\omega t_i}G^\pm(\mathbf{x}_R,\mathbf{x}_S^{(i)},\omega) \qquad (3)$$

where we refer to $s(\omega)$ as the source wavelet, G as the Green's function, and σ_S denotes a group of sources that emit signals at ignition times t_i closely following one after another, so that the responses are recorded with temporal overlap.

The integral along receivers in equation 1 can be discretised and written in a matrix form

$$\mathbf{p}^- = \mathbf{p}^+\mathbf{R}_0 \qquad (4)$$

Solving equation 4 for each frequency of interest in a least-squares sense is equivalent to solving its normal equation that are obtained by crosscorrelating both sides with $\mathbf{p}^{+}$ (e.g., Wapenaar et al., 2011)

$$\mathbf{R_0} = (\Gamma)^{\dagger}\,\mathbf{C} \qquad (5)$$

where $\Gamma=(\mathbf{p}^{+})^{H}\mathbf{p}^{+}$ represents the wavefield point-spread function (PSF) and $\mathbf{C}=(\mathbf{p}^{+})^{H}\mathbf{p}^{-}$ is called the correlation function, with H denoting the conjugate transpose matrix and † the regularised inverse (in this work $(\cdot)^{\dagger}=(\,\cdot+\varepsilon\mathbf{I})^{-1}$). Equation 5 states that the correlation function $\mathbf{C}$ is proportional to the desired response $\boldsymbol{R_0}$ smeared in space and time by Γ.

The existence of the relevant inverse operator for Γ is not guaranteed and its conditioning depends on many factors such as the number of available sources and receivers, the source and receiver array aperture, the source bandwidth, and the complexity of the velocity model. The so-called resolution matrix ($\delta = (\Gamma)^{\dagger}\,\Gamma$) can be introduced to diagnose the quality of the MDD process, with $\delta \rightarrow \mathbf{I}$ for all angular frequencies ω when the inversion is successful.

Demultiple (and deblending) of Volve OBC data

Volve is a oil field located in the gas/condensate-rich Sleipner area of the North Sea, offshore Norway. In 2002, a 3D OBC survey was acquired with a layout consisting of 12 cables and shot area of 12 km x 2.4 km. In this study we select a receiver line containing 235 receivers with an interval of 25 m and shot line composed of 241 sources with a shot interval of 50 m as shown in Figure 1a. Noise suppression, vector-fidelity corrections, and frequency filtering (to mitigate spatial aliasing in the data) are applied to the acquired data (e.g., pressure component in Figure 1b) before PZ summation.

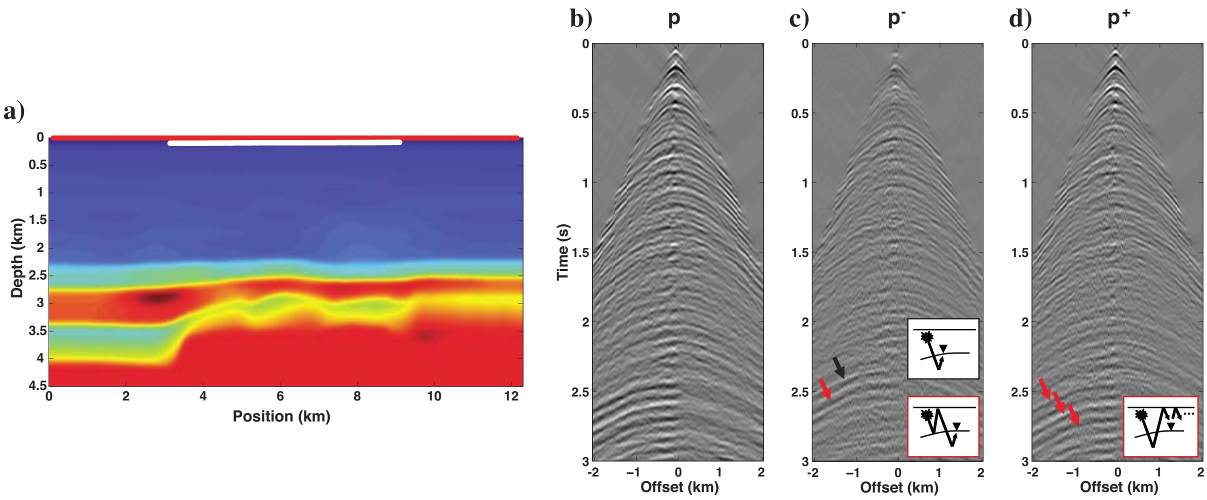

Figure 1 *a) Migration velocity model together with source (red line) and receiver (white line) locations. Common-shot gather (the initial 3s of the data are visualized) for a source at x_S=6km of a) full, b) up- and c) down-going pressure. Black arrow refers to a primary reflection event while source- and receiver-side free-surface multiple reflections are indicated by red arrows.*

Wavefield separation suppresses energy from receiver-side free-surface multiples (Figure 1d) in the up-going data. However source-side free-surface multiples remain along with primary reflections (Figure 1c). To remove also the effect of source-side multiple bounces before migration, the separated wavefields are transformed to the frequency domain and input to the demultiple (and deblending) approach. We generate two datasets to simulate simultaneous-source acquisitions by forming 60 source groups $\boldsymbol{\sigma_S}$ each containing four sources with ignition times chosen randomly from a uniform distribution between 0 and 1s. In the first case we combine four adjacent sources while in the second we combine sources 4km apart from each other. Multi-dimensional deconvolution of the up-going component with down-going component as in equation 5 successfully attenuates source-side free-surface multiples in the redatumed responses for both sequential (Figure 2a) and simultaneous-source acquisitions (Figures 2b and c): note, for example, that the source-side multiple just below the primary event at 2.5s in Figure 1c is successfully suppressed. Resolution matrices (Figures 2e, g, and i) further confirm the efficacy of the MDD approach, showing that most of the off-diagonal energy in the point-spread function has been removed by the inversion for each of the acquisition scenarios.

By comparing the point-spread functions from simultaneous sources for a frequency of 20 Hz (Figures 2f and h) with that from sequential sources (Figure 2d), we can explain the effect of source blending as an increase in the amplitude of off-diagonal values. This indicates that shot gathers from simultaneous sources are more correlated than those from sequential sources, thus providing a smaller amount of independent information that contributes to the retrieval of $\mathbf{R}_0$. While an in-depth study of the effect of matrix conditioning on the quality of estimates of $\mathbf{R}_0$ is beyond the scope of this work, we notice that adjacent simultaneous sources increase the power of off-diagonal values while keeping the same matrix structure as that from sequential sources, while distant simultaneous sources randomize the off-diagonal energy of the sequential matrix. These differences mainly reflect different levels of incoherent noise in the estimated $\mathbf{R}_0$.

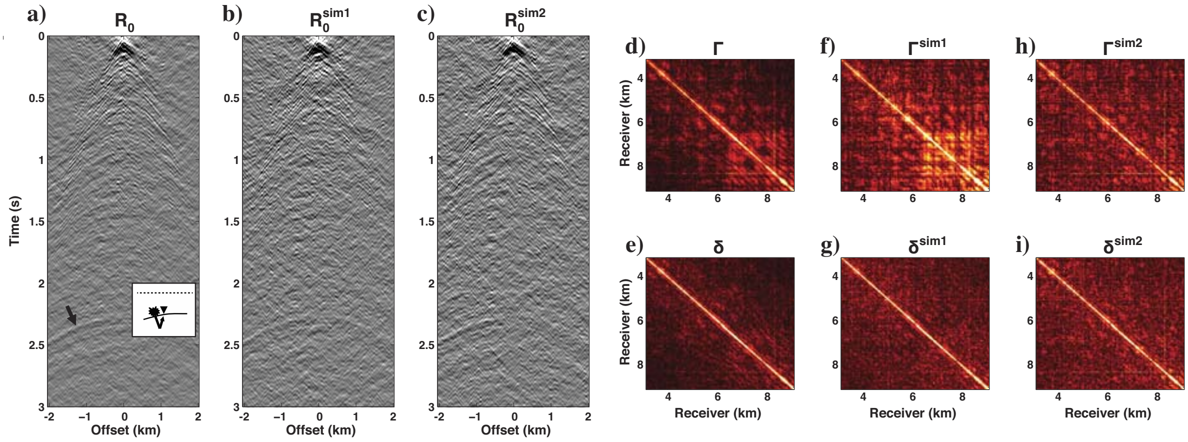

***Figure 2**. Common-shot gather of the desired redatumed response $\mathbf{R}_0$ for a source at x'_R=6km for a) sequential, b) adjacent simultaneous, and c) distant simultaneous sources. In the same order, d), f) and h) are point-spread functions and e), g) and i) are resolution matrices for a frequency of 20 Hz.*

Images are finally computed by means of reverse-time migration using the up-going component of the recorded data (Figure 1c) as well as the three different redatumed responses in Figure 2. Multiple events seen as up-going waves by the recorded array (e.g., source-side free-surface multiples) are incorrectly handled in migration of the up-going data and generate copies of the real interfaces (white arrow and white box in Figure 3a). In contrast, when the additional step of wave-equation demultiple is applied to data before migration, images do not show artefacts due to free-surface multiples. The quality of the images is very similar for sequential (Figure 3b) and simultaneous sources (Figure 3c and d) meaning that most of the additional incoherent noise in the redatumed responses has been stacked out by the imaging process.

Conclusion and discussion

The demultiple approach of Amundsen (2001) is a powerful processing step that can jointly suppress the effect of any type and order of free-surface multiples on both source- and receiver-side, apply source signature deconvolution (removing any residual phase in data), and deblend simultaneous-source data. Most implementations approximate multi-dimensional deconvolution of the up-going component with the down-going component by applying a deterministic trace-by-trace deconvolution in tau-p (or f-k) domain by assuming the geology to be horizontally layered (Mispel et al., 2007; Traub et al., 2009). We have instead shown that equation 1 can be successfully solved by direct matrix inversion thus accounting for the three-dimensional nature of the seismic wavefield and lateral heterogeneities in the shallow surface. While we have demonstrated that least-squares inversion works well on a 2D line of a real dataset, sparsity-promotion inversion (van der Neut and Herrmann, 2013) could represent an attractive alternative for 3D datasets, that is more robust to noise and artefacts due to coarse receiver sampling as is generally the case along the crossline direction.

Acknowledgements

The authors thank the Edinburgh Interferometry Project (EIP) sponsors (ConocoPhillips, Schlumberger Cambridge Research, Statoil and Total) for supporting this research. We also thank Statoil ASA and the Volve license partners ExxonMobil E&P Norway and Bayerngas Norge, for the release of the Volve data.

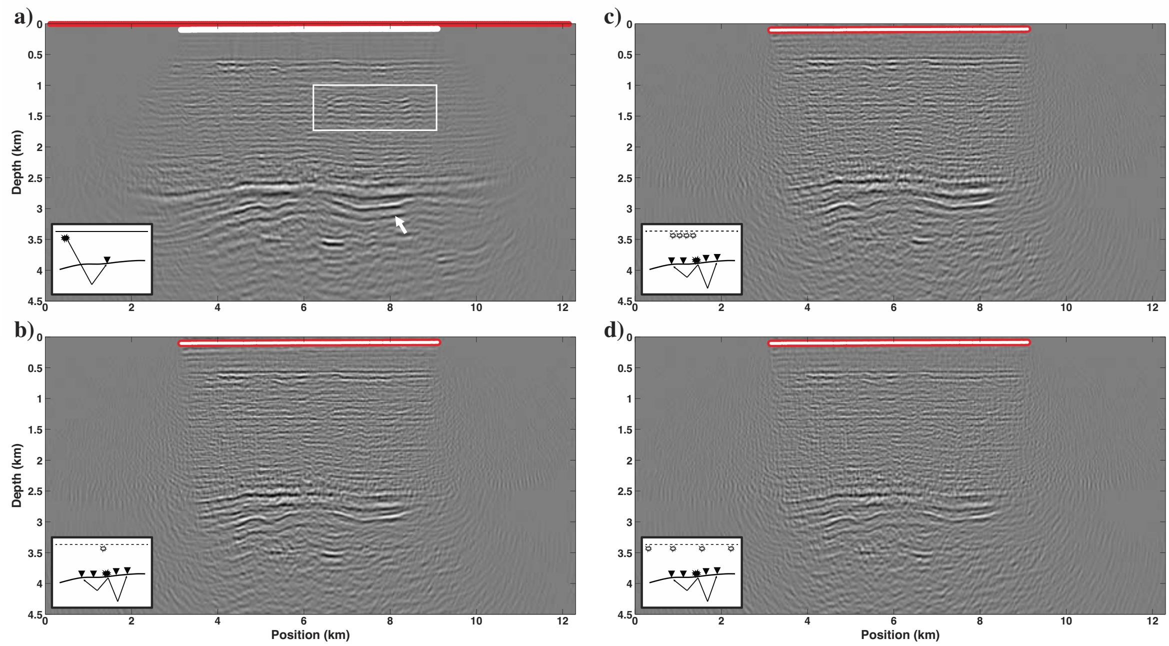

Figure 3 *Reverse-time migration of a) up-going field, and b), c) and d) redatumed responses from sequential, adjacent simultaneous, and distant simultaneous sources, respectively. A white arrow in a) indicates an artefact created from a source-side free-surface multiple. Other artefacts from the source-side free-surface multiples are visible in the white box in a).*

References

Amundsen, L. [2001] Elimination of free-surface related multiples without need of the source wavelet. Geophysics, **66**, (1), 327–341.

Barr, F. J., and Sanders, J. I. [1989] Attenuation of water-column multiples using pressure and velocity detectors in a water-bottom cable. SEG Technical Program Extended Abstracts.

El Yadari, N., and Hou, S. [2013] Vector-acoustic Kirchhoff Migration and its Mirror Extension – Theory and Examples. EAGE Conference & Exhibition Extended Abstracts.

Mispel, J., Arntsen, B., Kritski, A., Amundsen, L., Thompson, M., Sandvin, O., and Jahren, L. [2007] 3D multiple attenuation and depth imaging of ocean bottom seismic data. SEG Technical Program Extended Abstracts.

Ravasi, M., Vasconcelos, I., Curtis, A., and Kritski, A. [2014] Vector-Acoustic reverse-time migration of Volve OBC dataset without up/down decomposed wavefields. Second EAGE/SBGf Workshop 2014.

Soubaras, R. [1996] Ocean-bottom hydrophone and geophone processing. EAGE Conference & Exhibition Extended Abstracts.

Traub, B., Nguyen, A. K., and Riede, M [2009] Fast free surface multiples attenuation workflow for three-dimensional ocean bottom seismic data. Geophysical Prospecting, **57**, 785-802.

van der Neut, J., and Herrmann, F. J. [2013] Interferometric redatuming by sparse inversion. Geophysical Journal International, **192**, 666–670.

Vasconcelos, I. [2013] Source-receiver reverse-time imaging of dual-source, vector-acoustic seismic data. Geophysics, **78**, (2), WA147-WA

Vasconcelos I., and Rickett, J. [2013] Broadband extended images by joint inversion of multiple blended wavefields: Geophysics, **78**, WA147-WA158.

Wapenaar, K., van der Neut, J., Ruigrok, E., Draganov, D., Hunziker, J., Slob, E., Thorbecke, J., and Snieder, R. [2011] Seismic interferometry by crosscorrelation and by multi-dimensional deconvolution: a systematic comparison. Geophysical Journal International, **185**, 1335-1364.

Wapenaar, K., van der Neut, J., and Thorbecke, J., [2012] On the relation between seismic interferometry and the simultaneous-source method. Geophysical Journal International, **60**, 802-823.